

# Energy Dependence of Directed Flow in Au+Au Collisions from a Multi-phase Transport Model

J. Y. Chen\*

*Institution of Particle Physics, Huazhong Normal University(CCNU), Wuhan 430079, P.R.China and  
The Key Laboratory of Quark and Lepton Physics (Huazhong Normal University),  
Ministry of Education, Wuhan 430079, P.R.China*

J. X. Zuo†

*Institute of High Energy Physics, CAS, Beijing 100049, P.R.China*

X. Z. Cai

*Shanghai Institute of Applied Physics, CAS, Shanghai 201800, P.R.China*

F. Liu

*Institution of Particle Physics, Huazhong Normal University(CCNU), Wuhan 430079, P.R.China and  
The Key Laboratory of Quark and Lepton Physics (Huazhong Normal University),  
Ministry of Education, Wuhan 430079, P.R.China*

Y. G. Ma

*Shanghai Institute of Applied Physics, CAS, Shanghai 201800, P.R.China*

A. H. Tang

*Physics Department, Brookhaven National Lab., Upton, NY 11973, USA*

(Dated: November 5, 2018)

The directed flow of charged hadron and identified particles has been studied in the framework of a multi-phase transport (AMPT) model, for  $^{197}\text{Au}+^{197}\text{Au}$  collisions at  $\sqrt{s_{NN}}=200, 130, 62.4, 39, 17.2$  and  $9.2$  GeV. The rapidity, centrality and energy dependence of directed flow for charged particles over a wide rapidity range are presented. AMPT model gives the correct  $v_1(y)$  slope, as well as its trend as a function of energy, while it underestimates the magnitude. Within the AMPT model, the proton  $v_1$  slope is found to change its sign when the energy increases to 130 GeV - a feature that is consistent with “anti-flow”. Hadronic re-scattering is found having little effect on  $v_1$  at top RHIC energies. These studies can help us to understand the collective dynamics at early times in relativistic heavy-ion collisions, and they can also be served as references for the RHIC Beam Energy Scan program.

PACS numbers: 25.75.Ld, 25.75.Nq, 25.75.Dw

## I. INTRODUCTION

Anisotropic flow is one of the key observables in characterizing properties of the dense and hot medium created in the relativistic heavy-ion collisions[1]. It is quantified by Fourier coefficients when expanding particle’s azimuthal distribution with respect to the reaction plane[2]:

$$E \frac{d^3 N}{d^3 p} = \frac{1}{2\pi} \frac{d^2 N}{p_T dp_T dy} \left( 1 + \sum_{n=1}^{\infty} 2v_n \cos n\phi \right) \quad (1)$$

where  $\phi$  denotes the angle between the particle’s azimuthal angle in momentum space and the reaction plane angle. The sine terms in Fourier expansions vanish due to the reflection symmetry with respect to the reaction

plane. The various coefficients in this expansion can be defined as:

$$v_n = \langle \cos n\phi \rangle \quad (2)$$

The first and the second coefficients are named as directed flow ( $v_1$ ) and elliptic flow( $v_2$ ), respectively, and they play important roles in describing the collective expansion in azimuthal space. Elliptic flow is produced by the conversion of the initial coordinate-space anisotropy into momentum-space anisotropy, due to the developed large in-plane pressure gradient. Elliptic flow depends strongly on the re-scattering of the system constituents, thus it is sensitive to the degree of thermalization[3] of the system at early time. Directed flow, which is the focus of this study, describes the “side splash” of particles away from mid-rapidity[4], and it probes the dynamics of the system in the longitudinal direction. Since directed flow is generated very early, it brings information from the foremost early collective motion of the system. The

\*Electronic address: chenjy@iopp.ccnu.edu.cn

†Electronic address: zuojx@ihep.ac.cn

shapes of directed flow, in particular those for identified particles, are of special interest because they are sensitive to the equation of state (EOS) and may carry a phase transition signal[5].

The study of energy dependence of directed flow has implications in many aspects. Firstly, because directed flow has a unique, pre-equilibrium origin, it is expected to behave differently than other soft observables which show an “entropy-driven” multiplicity scaling[6]. It has been shown by STAR[7] that at top RHIC energies, directed flow is independent of system size, while it has an energy dependence. For a comprehensive study of the subject, it is necessary to extend the study of the energy dependence of directed flow in a wider energy range. Secondly, experiments at RHIC (PHENIX and STAR) have planned to look for the existence of the QCD phase boundary and the possible critical point by colliding heavy ions at various incident beam energies[8, 9, 10]. A non-monotonic dependence of variables on  $\sqrt{s_{NN}}$  and an increase in event-by-event fluctuations should become apparent near the critical point[8]. Directed flow is generated during the nuclear passage time ( $2R/\gamma \sim 0.1 fm/c$ ) and it probes the onset of bulk collective dynamics in the earlier stage of the collision. As a suggested signature of a first order phase transition[5], directed flow is sensitive to the creation of the critical point and it plays an important role in the proposed beam energy scan program.

In this paper, directed flow from the AMPT model for 6 energies are presented. They are, 9.2, 17.3, 39, 62.4, 130 and 200 GeV. The comparison with the measurements from STAR and PHOBOS are made at top energies. The particle type dependence over a wide rapidity range is discussed. This study will deepen our understanding about the energy dependence of directed flow, and it can be also served as a valuable reference for the RHIC Beam Energy Scan program.

## II. THE AMPT MODEL

The AMPT model consists of four main components[11]: initial conditions, partonic interactions, conversion from partonic matter to hadronic matter, and hadronic interactions. The initial conditions, which include the spatial and momentum distributions of the mini-jet partons and soft string excitations, are obtained from the HIJING model[13]. The scatterings among partons are modeled by Zhang’s parton cascade(ZPC)[14], which includes two-body scatterings with cross sections from pQCD with screening masses. In the default AMPT model[15], partons are recombined with their parent strings when they stop interacting, and the resulting strings fragment into hadrons according to the Lund string fragmentation model[16]. In the AMPT model with string melting[17], quark coalescence is used instead to combine partons into hadrons. The dynamics of the subsequent hadronic matter is described by the ART (a relativistic transport)

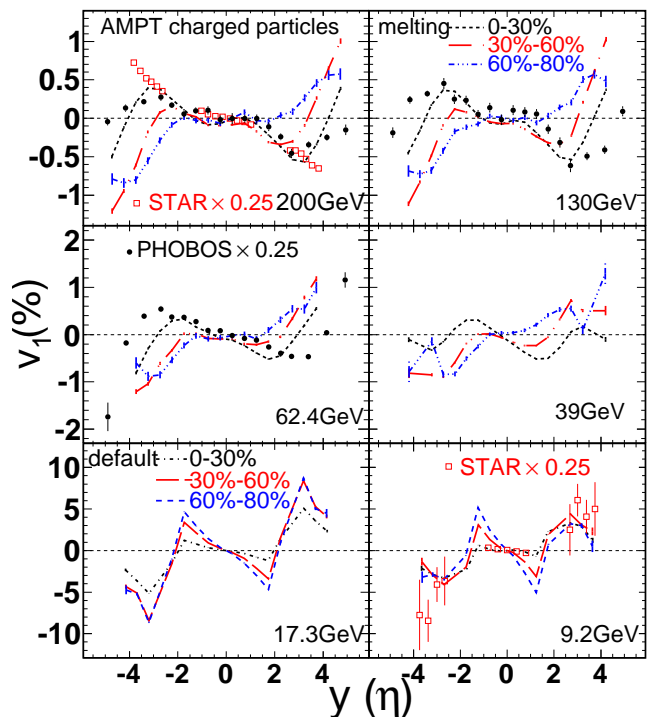


FIG. 1: Rapidity dependence of  $v_1$  for charged particles in the AMPT model compared with STAR and PHOBOS data (plotted as a function of  $\eta$ ) in the Au+Au collisions at  $\sqrt{s_{NN}} = 200$  GeV. The dashed lines showed AMPT result from different centrality: 0-30%(black), 30%-60%(red), 60%-80%(blue).

model[18] with modifications and extensions. As suggested in Ref.[19], the parton cross section is chosen as 3 mb in our analysis. All the errors presented here are statistical only.

## III. ANALYSIS AND RESULTS

In Fig. 1, the directed flow of charged particles from AMPT is shown as a function of rapidity, for collision energies of 200, 130, 62.4, 39, 17.2 and 9.2 GeV. The centrality is divided into three bins, namely, 0-30%, 30%-60% and 60%-80%, based on the impact parameter ( $b$ ) distribution. The calculations with string melting scenario is used for high energies (200, 130, 62.4, 39 GeV) while for low energies (17.2 and 9.2 GeV) calculations are performed with default scenario. The reason for such choice is because that, it is argued [19, 20, 21] that the string melting should be used to explain flow around midrapidity at top RHIC energies, and default setting describes data at 9.2 GeV the best. The energy density in the collisions at the RHIC top energies is much higher than the critical density for the QCD phase transition. More discussion on different AMPT configurations can be found later in this paper. All results are obtained by integrating

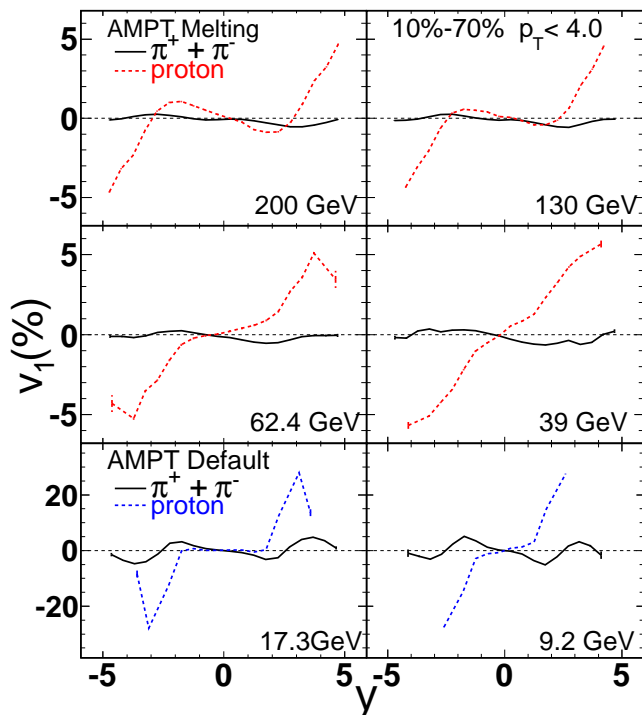


FIG. 2: Proton (solid lines) and Pion (dashed lines)  $v_1(y)$  from AMPT at centrality 10%-70%.

over transverse momentum ( $p_T$ ) up to 4.0 GeV/c. Experimental results from STAR[7, 22] and PHOBOS[23] are also shown for comparison. The charged hadron  $v_1$  measured by the PHOBOS experiment is for 0-40% central collisions, and the results measured by STAR experiment are for centrality 30%-60% at 200GeV, and centrality 0-60% at 9.2GeV. In general, AMPT gives larger  $v_1$  at low energies than at high energies, the same trend has been seen in data. At top RHIC energies, AMPT underestimated  $v_1$ , due to the turn-off of mean-field potentials in ART when implemented in AMPT to describe the hadronic scattering[11]. However, in the rapidity range of  $[-2.0, 2.0]$ , the shape of  $v_1$  between AMPT calculations and experimental data are in good agreement – this can be seen by scaling experimental results with a factor of 0.25.

The particle type dependence of directed flow is shown in Fig. 2. The different sign of  $v_1$  between pions and protons at low energies can be understood as nucleon shadowing and baryon stopping[24, 25]. In general the magnitude of the  $v_1$  slope at midrapidity decreases with increasing energy. This effect is most profound for protons, for which the slope keeps decreasing and when the energy is high enough, it changes its sign and protons begin to flow together with pions. This is consistent with the “anti-flow” scenario[26], in which the “bounce-off” motion and transverse expansion of nucleons compete with each other around midrapidity, and when the transverse expansion is strong enough (e.g., at top RHIC energies), it overcomes the “bounce-off” motion and causes

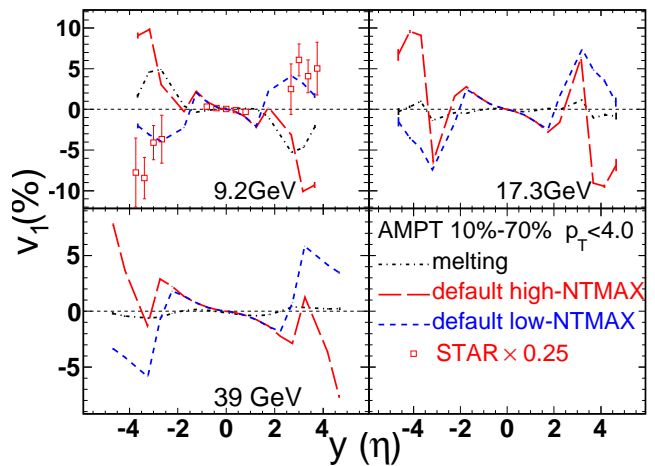


FIG. 3: Charged particles  $v_1(y)$  from centrality 10%-70% for 9.2GeV (upper left panel), 17.3GeV (upper right panel) and 39GeV (down left panel). The dashed lines show three AMPT versions: string melting scenario (black), default scenario with high-NTMAX (red) and low-NTMAX (blue). Experimental data points from STAR are plotted as a function of  $\eta$ .

protons to change their sign of directed flow.

To illustrate the effect on  $v_1$  due to different configurations in AMPT, in Fig. 3 we present the directed flow of charged hadrons in low energy collisions, from AMPT calculations with the string melting scenario and the default scenario. The similar study for higher energies can be found in [19]. The calculation with string melting yields the smallest  $v_1$  slope around midrapidity and is close to data. Two different default scenarios are also studied: one is calculated with NTMAX=2500 (high-NTMAX), and the other, NTMAX=150 (low-NTMAX). NTMAX stands for the number of time-steps for the hadron cascade (see detail in paper [11]). A large NTMAX means a thoroughly developed hadron cascade, as  $0.2\text{fm}/c \cdot \text{NTMAX}$  is the termination time, in the center of mass frame, of the hadron cascade in AMPT model. The comparison, for low energies, of  $v_1$  calculated between low-NTMAX and high-NTMAX indicates that  $v_1$  can change its sign at large rapidity if the time for the hadronic cascade is long enough. In default AMPT, the NTMAX has to be much larger than 150 in order to describe  $v_1$  at large rapidity. The disagreement between the experimental data and the calculation made with high-NTMAX is mostly due to the lack of the mean-field in the hadron cascade in AMPT, which is a considerable effect at low energies when the nuclei passage time is not negligible (compared to that at high energies). The AMPT calculation with high-NTMAX at high energy has been presented in [12]. In this paper, we address the comparison around midrapidity only, and results presented in this paper are made with low-NTMAX unless otherwise specified.

The energy dependence of charged particle directed flow, calculated with the AMPT model, is shown in

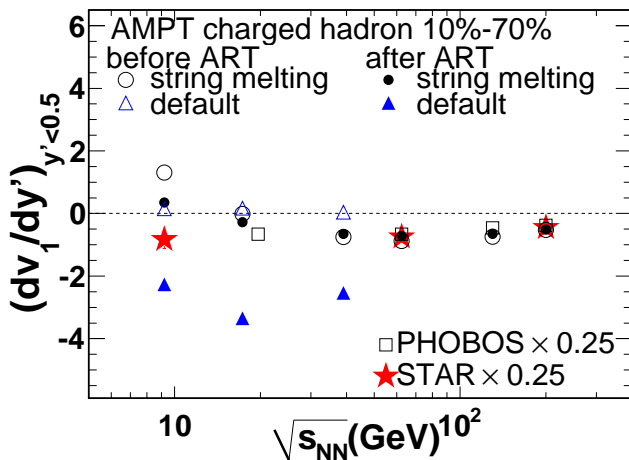


FIG. 4: Charged hadrons' slope  $dv_1/dy'$  in the mid-rapidity  $|y'| < 0.5$  as a function of incident-energy. The data are taken from STAR(stars) and PHOBOS(squares) and scaled by a factor 0.25. The AMPT calculations with string melting before ART are depicted with open circles and after hadron cascade are depicted with full circles. The open triangles depict the default AMPT calculations before ART and the full triangles depict after hadron cascade.

Fig. 4. Experimental data are also shown for comparison. The centrality for which the calculation is performed is 10%-70%. The centrality for PHOBOS data from different energies is 0-40% while the centrality selection for STAR data are 0-60% for 9.2 GeV, 10%-70% for 62.4 GeV, and 30%-60% for 200 GeV. To obtain the integrated  $v_1$ , one needs to fold in the spectra at different energies, which brings in an additional layer of systematics. Thus instead, we present the slope of  $v_1(y)$  around mid-rapidity ( $|y'| < 0.5$ ) extracted from the normalized ( $y' = y/y_{beam}$ ) rapidity distribution, where  $y_{beam}$  is the beam rapidity. For the energy range that string melting is used (39 GeV and above), all the AMPT calculations underestimate the experimental data, however, they predict the right trend of the energy dependence. For the low energies at 9.2 GeV, calculations with string melting did a poor job, the calculation with the default AMPT

improves the result in the right direction yet is still not be able to explain the data. The hadron re-scattering effect on directed flow  $v_1$  can be seen by switching off the hadron cascade in the AMPT calculation. Comparing the difference between the result with hadron cascade (open symbols) and without (solid symbols), it is found that the hadronic cascade has a significant effect for low energy results but little for that of high energies. This can be understood as that, when the energy is high enough, the hadron re-scattering become less important due to the presence of strong collective motion built up beforehand.

#### IV. SUMMARY AND CONCLUSIONS

In this paper,  $v_1$  values calculated from the AMPT model for different energies are discussed. It is found that the AMPT model gives the right shape of  $v_1$  versus  $y$  while underestimating the magnitude, possibly due to the lack of mean-field in its hadron cascade. In AMPT, the proton  $v_1$  slope changes its sign when the energy increases to 130 GeV and begins to have the same sign as that of pions, as expected in the "anti-flow" scenario. The effect on  $v_1$  due to string melting, low-NTMAX and high-NTMAX are illustrated. The energy dependence of the  $v_1$  slope at midrapidity is compared to experimental data, and AMPT can describe the trend of energy dependence while missing the magnitude by a fraction of 75%. Hadronic rescattering is found to be less important at high energies as the strong collective motion becomes to be the dominant dynamics.

#### Acknowledgments

Authors greatly thank Zi-Wei Lin and Zhangbu Xu for useful discussions and kindly providing comments to this paper. Authors appreciate Matthew Lamont's help on English QA. This work was supported in part the National Natural Science Foundation of China under Grant No. 10775058 & No. 10610285, MOE of China under Grant No. IRT0624 and MOST of China under Grant No. 2008CB817707, and the Knowledge Innovation Project of the Chinese Academy of Sciences under Grant Nos. KJCX2-YW-A14 and and KJCX3-SYW-N2.

[1] For a recent review, see : S. A. Voloshin, A. M. Poskanzer and R. Snellings, arXiv: 0909.2949 [nucl-ex].  
[2] A. M. Poskanzer and S. A. Voloshin, Phys. Rev. C **58** 1671 (1998).  
[3] P. Kolb, J. Sollfrank, and U. Heinz, Phys. Rev. C **62** 054909 (2000).  
[4] H. Sorge, Phys. Rev. Lett. **78** 2309 (1997).  
[5] H. Stöcker, Nucl. Phys. A **750** 121-147 (2005).  
[6] A. H. Tang, J. Phys. G **34**, S277 (2007); H. Song and U. Heinz, Phys. Rev. C **78** 024902 (2008); J. Chen (for the STAR Collaboration) J. Phys. G **35** 044072 (2008).

[7] B. I. Abelev *et al.* (STAR experiment), Phys. Rev. Lett. **101** 252301 (2008).  
[8] P. Sorensen (for STAR Collaboration), PoS CPOD **019** (2006), arXiv: 0701028v1 [nucl-ex].  
[9] G. Odyniec (for STAR Collaboration), J. Phys. G **35** 104164 (2008).  
[10] T. Sakaguchi (for PHENIX Collaboration), PHENIX plans for RHIC low energy run, talk for the 5th International Workshop on Critical Point and Onset of Deconfinement (CPOD), [[http://quark.phy.bnl.gov/~karsch/agenda\\_cpod.html](http://quark.phy.bnl.gov/~karsch/agenda_cpod.html)].

- [11] Z. W. Lin, C. M. Ko, B. A. Li, B. Zhang, and S. Pal, Phys. Rev. C **72** 064901 (2005).
- [12] L. W. Chen, V. Greco, C. M. Ko and P. Kolb, Phys. Lett. B **605** 95 (2005).
- [13] X. N. Wang and M. Gyulassy, Phys. Rev. D **45** 844 (1992); M. Gyulassy and X. N. Wang, Comput. Phys. Commun. **83** 307 (1994).
- [14] B. Zhang, Comput. Phys. Commun. **109** 193 (1998).
- [15] Z. W. Lin and C. M. Ko, Phys. Rev. C **68** 054904 (2003).
- [16] B. Andersson, G. Gustafson and B. Soderbery, Z. Phys. C **20** 317 (1983).
- [17] Z. W. Lin and C. M. Ko, J. Phys. G **30** S263 (2004).
- [18] B. Li, A. T. Sustich, B. Zhang and C. M. Ko, Int. J. Mod. Phys. E **10** 267 (2001).
- [19] C. M. Ko and L. W. Chen Nucl. Phys. A **774** 527 (2006).
- [20] J. H. Chen et.al Phys. Rev. C **74** 064902 (2006).
- [21] J. X. Zuo et.al Eur. Phys. J. C **55** 463 (2008).
- [22] B. I. Abelev *et al.* (STAR Collaboration), arXiv: 0909.4131 [nucl-ex]; L. Kumar (for the STAR Collaboration) J. Phys. G **36** 064066 (2009); J. Y. Chen (for STAR Collaboration), arXiv: 0910.0556 [nucl-ex].
- [23] B. B. Back *et al.* (PHOBOS Collaboration), Phys. Rev. Lett. **97** 012301 (2006).
- [24] R. J. M. Snellings, H. Sorge, S. A. Voloshin, F. Q. Wang, and N. Xu, Phys. Rev. Lett. **84** 2803 (2000).
- [25] H. Liu, S. Panitkin and N. Xu, Phys. Rev. C **59** 348 (1998).
- [26] J. Brachmann *et al.*, Phys. Rev. C **61** 024909 (2000); L.P. Csernai and D.Rohrich, Phys. Lett. B **458** 454 (1999).

# Energy Dependence of Directed Flow in Au+Au Collisions from a Multi-phase Transport Model

J. Y. Chen\*

*Institution of Particle Physics, Huazhong Normal University(CCNU), Wuhan 430079, P.R.China and  
The Key Laboratory of Quark and Lepton Physics (Huazhong Normal University),  
Ministry of Education, Wuhan 430079, P.R.China*

J. X. Zuo†

*Institute of High Energy Physics, CAS, Beijing 100049, P.R.China*

X. Z. Cai

*Shanghai Institute of Applied Physics, CAS, Shanghai 201800, P.R.China*

F. Liu

*Institution of Particle Physics, Huazhong Normal University(CCNU), Wuhan 430079, P.R.China and  
The Key Laboratory of Quark and Lepton Physics (Huazhong Normal University),  
Ministry of Education, Wuhan 430079, P.R.China*

Y. G. Ma

*Shanghai Institute of Applied Physics, CAS, Shanghai 201800, P.R.China*

A. H. Tang

*Physics Department, Brookhaven National Lab., Upton, NY 11973, USA*

(Dated: November 5, 2018)

The directed flow of charged hadron and identified particles has been studied in the framework of a multi-phase transport (AMPT) model, for  $^{197}\text{Au}+^{197}\text{Au}$  collisions at  $\sqrt{s_{NN}}=200, 130, 62.4, 39, 17.2$  and  $9.2$  GeV. The rapidity, centrality and energy dependence of directed flow for charged particles over a wide rapidity range are presented. AMPT model gives the correct  $v_1(y)$  slope, as well as its trend as a function of energy, while it underestimates the magnitude. Within the AMPT model, the proton  $v_1$  slope is found to change its sign when the energy increases to 130 GeV - a feature that is consistent with “anti-flow”. Hadronic re-scattering is found having little effect on  $v_1$  at top RHIC energies. These studies can help us to understand the collective dynamics at early times in relativistic heavy-ion collisions, and they can also be served as references for the RHIC Beam Energy Scan program.

PACS numbers: 25.75.Ld, 25.75.Nq, 25.75.Dw

## I. INTRODUCTION

Anisotropic flow is one of the key observables in characterizing properties of the dense and hot medium created in the relativistic heavy-ion collisions[1]. It is quantified by Fourier coefficients when expanding particle’s azimuthal distribution with respect to the reaction plane[2]:

$$E \frac{d^3 N}{d^3 p} = \frac{1}{2\pi} \frac{d^2 N}{p_T dp_T dy} \left( 1 + \sum_{n=1}^{\infty} 2v_n \cos n\phi \right) \quad (1)$$

where  $\phi$  denotes the angle between the particle’s azimuthal angle in momentum space and the reaction plane angle. The sine terms in Fourier expansions vanish due to the reflection symmetry with respect to the reaction

plane. The various coefficients in this expansion can be defined as:

$$v_n = \langle \cos n\phi \rangle \quad (2)$$

The first and the second coefficients are named as directed flow ( $v_1$ ) and elliptic flow( $v_2$ ), respectively, and they play important roles in describing the collective expansion in azimuthal space. Elliptic flow is produced by the conversion of the initial coordinate-space anisotropy into momentum-space anisotropy, due to the developed large in-plane pressure gradient. Elliptic flow depends strongly on the re-scattering of the system constituents, thus it is sensitive to the degree of thermalization[3] of the system at early time. Directed flow, which is the focus of this study, describes the “side splash” of particles away from mid-rapidity[4], and it probes the dynamics of the system in the longitudinal direction. Since directed flow is generated very early, it brings information from the foremost early collective motion of the system. The

\*Electronic address: chenjy@iopp.cnu.edu.cn

†Electronic address: zuojx@ihep.ac.cn

shapes of directed flow, in particular those for identified particles, are of special interest because they are sensitive to the equation of state (EOS) and may carry a phase transition signal[5].

The study of energy dependence of directed flow has implications in many aspects. Firstly, because directed flow has a unique, pre-equilibrium origin, it is expected to behave differently than other soft observables which show an “entropy-driven” multiplicity scaling[6]. It has been shown by STAR[7] that at top RHIC energies, directed flow is independent of system size, while it has an energy dependence. For a comprehensive study of the subject, it is necessary to extend the study of the energy dependence of directed flow in a wider energy range. Secondly, experiments at RHIC (PHENIX and STAR) have planned to look for the existence of the QCD phase boundary and the possible critical point by colliding heavy ions at various incident beam energies[8, 9, 10]. A non-monotonic dependence of variables on  $\sqrt{s_{NN}}$  and an increase in event-by-event fluctuations should become apparent near the critical point[8]. Directed flow is generated during the nuclear passage time ( $2R/\gamma \sim 0.1 fm/c$ ) and it probes the onset of bulk collective dynamics in the earlier stage of the collision. As a suggested signature of a first order phase transition[5], directed flow is sensitive to the creation of the critical point and it plays an important role in the proposed beam energy scan program.

In this paper, directed flow from the AMPT model for 6 energies are presented. They are, 9.2, 17.3, 39, 62.4, 130 and 200 GeV. The comparison with the measurements from STAR and PHOBOS are made at top energies. The particle type dependence over a wide rapidity range is discussed. This study will deepen our understanding about the energy dependence of directed flow, and it can be also served as a valuable reference for the RHIC Beam Energy Scan program.

## II. THE AMPT MODEL

The AMPT model consists of four main components[11]: initial conditions, partonic interactions, conversion from partonic matter to hadronic matter, and hadronic interactions. The initial conditions, which include the spatial and momentum distributions of the mini-jet partons and soft string excitations, are obtained from the HIJING model[13]. The scatterings among partons are modeled by Zhang’s parton cascade(ZPC)[14], which includes two-body scatterings with cross sections from pQCD with screening masses. In the default AMPT model[15], partons are recombined with their parent strings when they stop interacting, and the resulting strings fragment into hadrons according to the Lund string fragmentation model[16]. In the AMPT model with string melting[17], quark coalescence is used instead to combine partons into hadrons. The dynamics of the subsequent hadronic matter is described by the ART (a relativistic transport)

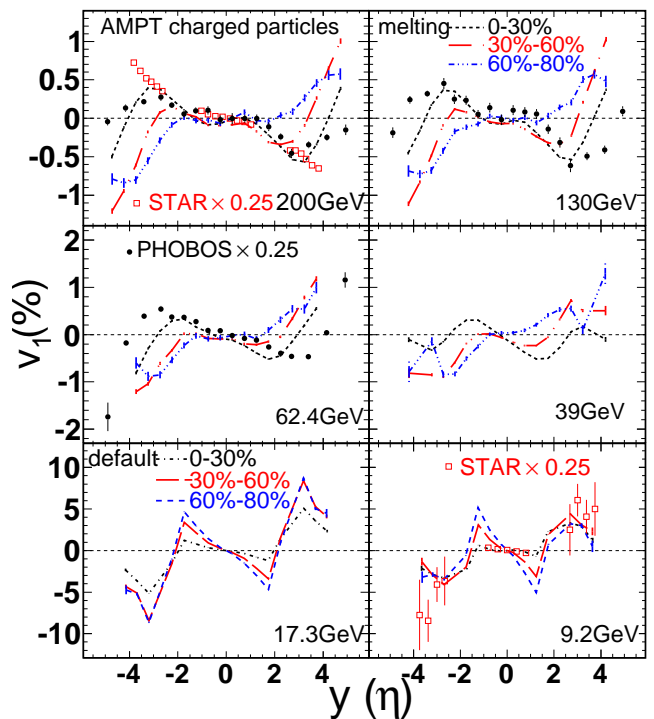


FIG. 1: Rapidity dependence of  $v_1$  for charged particles in the AMPT model compared with STAR and PHOBOS data (plotted as a function of  $\eta$ ) in the Au+Au collisions at  $\sqrt{s_{NN}} = 200$  GeV. The dashed lines showed AMPT result from different centrality: 0-30%(black), 30%-60%(red), 60%-80%(blue).

model[18] with modifications and extensions. As suggested in Ref.[19], the parton cross section is chosen as 3 mb in our analysis. All the errors presented here are statistical only.

## III. ANALYSIS AND RESULTS

In Fig. 1, the directed flow of charged particles from AMPT is shown as a function of rapidity, for collision energies of 200, 130, 62.4, 39, 17.2 and 9.2 GeV. The centrality is divided into three bins, namely, 0-30%, 30%-60% and 60%-80%, based on the impact parameter ( $b$ ) distribution. The calculations with string melting scenario is used for high energies (200, 130, 62.4, 39 GeV) while for low energies (17.2 and 9.2 GeV) calculations are performed with default scenario. The reason for such choice is because that, it is argued [19, 20, 21] that the string melting should be used to explain flow around midrapidity at top RHIC energies, and default setting describes data at 9.2 GeV the best. The energy density in the collisions at the RHIC top energies is much higher than the critical density for the QCD phase transition. More discussion on different AMPT configurations can be found later in this paper. All results are obtained by integrating

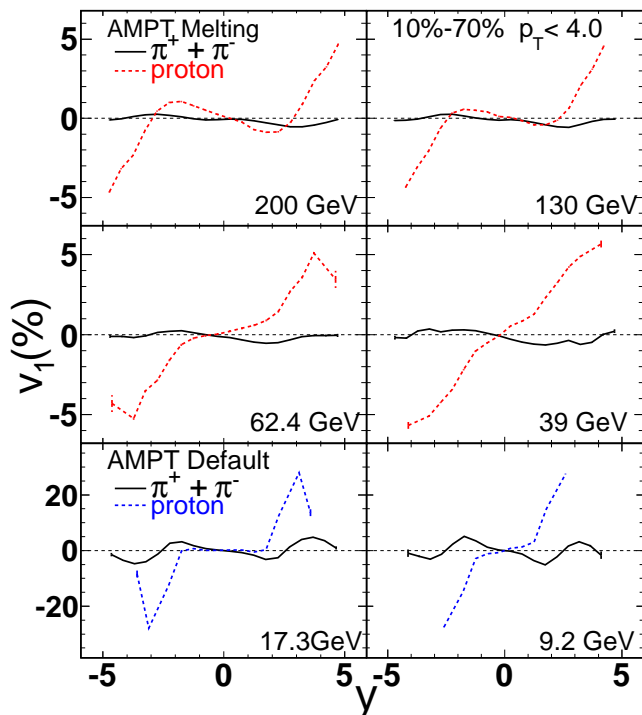


FIG. 2: Proton (solid lines) and Pion (dashed lines)  $v_1(y)$  from AMPT at centrality 10%-70%.

over transverse momentum ( $p_T$ ) up to 4.0 GeV/c. Experimental results from STAR[7, 22] and PHOBOS[23] are also shown for comparison. The charged hadron  $v_1$  measured by the PHOBOS experiment is for 0-40% central collisions, and the results measured by STAR experiment are for centrality 30%-60% at 200GeV, and centrality 0-60% at 9.2GeV. In general, AMPT gives larger  $v_1$  at low energies than at high energies, the same trend has been seen in data. At top RHIC energies, AMPT underestimated  $v_1$ , due to the turn-off of mean-field potentials in ART when implemented in AMPT to describe the hadronic scattering[11]. However, in the rapidity range of  $[-2.0, 2.0]$ , the shape of  $v_1$  between AMPT calculations and experimental data are in good agreement – this can be seen by scaling experimental results with a factor of 0.25.

The particle type dependence of directed flow is shown in Fig. 2. The different sign of  $v_1$  between pions and protons at low energies can be understood as nucleon shadowing and baryon stopping[24, 25]. In general the magnitude of the  $v_1$  slope at midrapidity decreases with increasing energy. This effect is most profound for protons, for which the slope keeps decreasing and when the energy is high enough, it changes its sign and protons begin to flow together with pions. This is consistent with the “anti-flow” scenario[26], in which the “bounce-off” motion and transverse expansion of nucleons compete with each other around midrapidity, and when the transverse expansion is strong enough (e.g., at top RHIC energies), it overcomes the “bounce-off” motion and causes

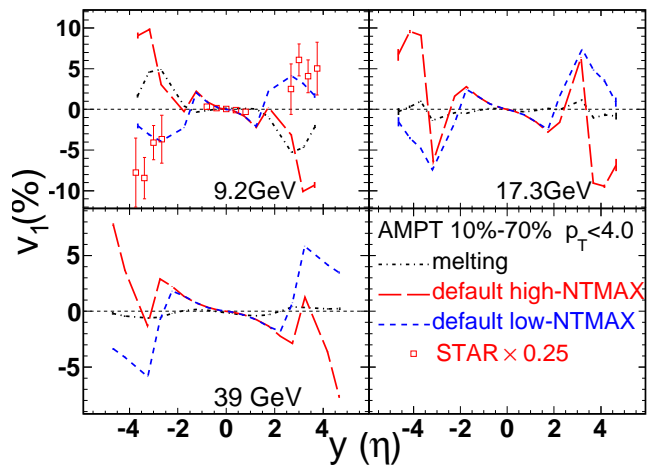


FIG. 3: Charged particles  $v_1(y)$  from centrality 10%-70% for 9.2GeV (upper left panel), 17.3GeV (upper right panel) and 39GeV (down left panel). The dashed lines show three AMPT versions: string melting scenario (black), default scenario with high-NTMAX (red) and low-NTMAX (blue). Experimental data points from STAR are plotted as a function of  $\eta$ .

protons to change their sign of directed flow.

To illustrate the effect on  $v_1$  due to different configurations in AMPT, in Fig. 3 we present the directed flow of charged hadrons in low energy collisions, from AMPT calculations with the string melting scenario and the default scenario. The similar study for higher energies can be found in [19]. The calculation with string melting yields the smallest  $v_1$  slope around mid-rapidity and is close to data. Two different default scenarios are also studied: one is calculated with NTMAX=2500 (high-NTMAX), and the other, NTMAX=150 (low-NTMAX). NTMAX stands for the number of time-steps for the hadron cascade (see detail in paper [11]). A large NTMAX means a thoroughly developed hadron cascade, as  $0.2\text{fm}/c \cdot \text{NTMAX}$  is the termination time, in the center of mass frame, of the hadron cascade in AMPT model. The comparison, for low energies, of  $v_1$  calculated between low-NTMAX and high-NTMAX indicates that  $v_1$  can change its sign at large rapidity if the time for the hadronic cascade is long enough. In default AMPT, the NTMAX has to be much larger than 150 in order to describe  $v_1$  at large rapidity. The disagreement between the experimental data and the calculation made with high-NTMAX is mostly due to the lack of the mean-field in the hadron cascade in AMPT, which is a considerable effect at low energies when the nuclei passage time is not negligible (compared to that at high energies). The AMPT calculation with high-NTMAX at high energy has been presented in [12]. In this paper, we address the comparison around midrapidity only, and results presented in this paper are made with low-NTMAX unless otherwise specified.

The energy dependence of charged particle directed flow, calculated with the AMPT model, is shown in

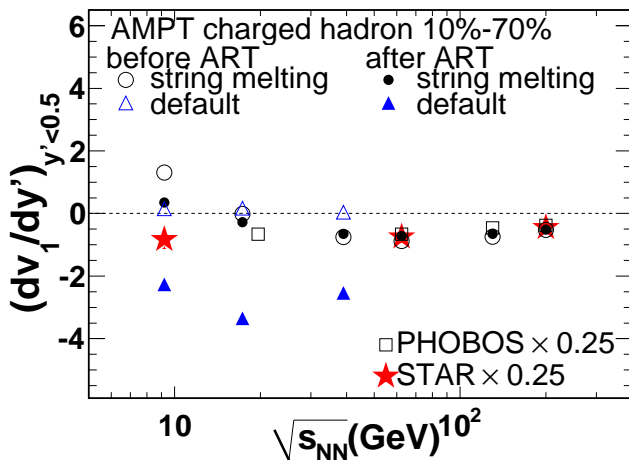


FIG. 4: Charged hadrons' slope  $dv_1/dy'$  in the mid-rapidity  $|y'| < 0.5$  as a function of incident-energy. The data are taken from STAR(stars) and PHOBOS(squares) and scaled by a factor 0.25. The AMPT calculations with string melting before ART are depicted with open circles and after hadron cascade are depicted with full circles. The open triangles depict the default AMPT calculations before ART and the full triangles depict after hadron cascade.

Fig. 4. Experimental data are also shown for comparison. The centrality for which the calculation is performed is 10%-70%. The centrality for PHOBOS data from different energies is 0-40% while the centrality selection for STAR data are 0-60% for 9.2 GeV, 10%-70% for 62.4 GeV, and 30%-60% for 200 GeV. To obtain the integrated  $v_1$ , one needs to fold in the spectra at different energies, which brings in an additional layer of systematics. Thus instead, we present the slope of  $v_1(y)$  around mid-rapidity ( $|y'| < 0.5$ ) extracted from the normalized ( $y' = y/y_{beam}$ ) rapidity distribution, where  $y_{beam}$  is the beam rapidity. For the energy range that string melting is used (39 GeV and above), all the AMPT calculations underestimate the experimental data, however, they predict the right trend of the energy dependence. For the low energies at 9.2 GeV, calculations with string melting did a poor job, the calculation with the default AMPT

improves the result in the right direction yet is still not be able to explain the data. The hadron re-scattering effect on directed flow  $v_1$  can be seen by switching off the hadron cascade in the AMPT calculation. Comparing the difference between the result with hadron cascade (open symbols) and without (solid symbols), it is found that the hadronic cascade has a significant effect for low energy results but little for that of high energies. This can be understood as that, when the energy is high enough, the hadron re-scattering become less important due to the presence of strong collective motion built up beforehand.

#### IV. SUMMARY AND CONCLUSIONS

In this paper,  $v_1$  values calculated from the AMPT model for different energies are discussed. It is found that the AMPT model gives the right shape of  $v_1$  versus  $y$  while underestimating the magnitude, possibly due to the lack of mean-field in its hadron cascade. In AMPT, the proton  $v_1$  slope changes its sign when the energy increases to 130 GeV and begins to have the same sign as that of pions, as expected in the "anti-flow" scenario. The effect on  $v_1$  due to string melting, low-NTMAX and high-NTMAX are illustrated. The energy dependence of the  $v_1$  slope at midrapidity is compared to experimental data, and AMPT can describe the trend of energy dependence while missing the magnitude by a fraction of 75%. Hadronic rescattering is found to be less important at high energies as the strong collective motion becomes to be the dominant dynamics.

#### Acknowledgments

Authors greatly thank Zi-Wei Lin and Zhangbu Xu for useful discussions and kindly providing comments to this paper. Authors appreciate Matthew Lamont's help on English QA. This work was supported in part the National Natural Science Foundation of China under Grant No. 10775058 & No. 10610285, MOE of China under Grant No. IRT0624 and MOST of China under Grant No. 2008CB817707, and the Knowledge Innovation Project of the Chinese Academy of Sciences under Grant Nos. KJCX2-YW-A14 and and KJCX3-SYW-N2.

[1] For a recent review, see : S. A. Voloshin, A. M. Poskanzer and R. Snellings, arXiv: 0909.2949 [nucl-ex].  
 [2] A. M. Poskanzer and S. A. Voloshin, Phys. Rev. C **58** 1671 (1998).  
 [3] P. Kolb, J. Sollfrank, and U. Heinz, Phys. Rev. C **62** 054909 (2000).  
 [4] H. Sorge, Phys. Rev. Lett. **78** 2309 (1997).  
 [5] H. Stöcker, Nucl. Phys. A **750** 121-147 (2005).  
 [6] A. H. Tang, J. Phys. G **34**, S277 (2007); H. Song and U. Heinz, Phys. Rev. C **78** 024902 (2008); J. Chen (for the STAR Collaboration) J. Phys. G **35** 044072 (2008).

[7] B. I. Abelev *et al.* (STAR experiment), Phys. Rev. Lett. **101** 252301 (2008).  
 [8] P. Sorensen (for STAR Collaboration) PoS CPOD (019),2006, arXiv: 0701028v1 [nucl-ex].  
 [9] G. Odyniec (for STAR Collaboration), J. Phys. G **35** 104164 (2008).  
 [10] T. Sakaguchi (for PHENIX Collaboration), PHENIX plans for RHIC low energy run, talk for the 5th International Workshop on Critical Point and Onset of Deconfinement (CPOD), [[http://quark.phy.bnl.gov/~karsch/agenda\\_cpod.html](http://quark.phy.bnl.gov/~karsch/agenda_cpod.html)].

- [11] Z. W. Lin, C. M. Ko, B. A. Li, B. Zhang, and S. Pal, Phys. Rev. C **72** 064901 (2005).
- [12] L. W. Chen, V. Greco, C. M. Ko and P. Kolb, Phys. Lett. B **605** 95 (2005).
- [13] X. N. Wang and M. Gyulassy, Phys. Rev. D **45** 844 (1992); M. Gyulassy and X. N. Wang, Comput. Phys. Commun. **83** 307 (1994).
- [14] B. Zhang, Comput. Phys. Commun. **109** 193 (1998).
- [15] Z. W. Lin and C. M. Ko, Phys. Rev. C **68** 054904 (2003).
- [16] B. Andersson, G. Gustafson and B. Soderbery, Z. Phys. C **20** 317 (1983).
- [17] Z. W. Lin and C. M. Ko, J. Phys. G **30** S263 (2004).
- [18] B. Li, A. T. Sustich, B. Zhang and C. M. Ko, Int. J. Mod. Phys. E **10** 267 (2001).
- [19] C. M. Ko and L. W. Chen Nucl. Phys. A **774** 527 (2006).
- [20] J. H. Chen et.al Phys. Rev. C **74** 064902 (2006).
- [21] J. X. Zuo et.al Eur. Phys. J. C **55** 463 (2008).
- [22] B. I. Abelev *et al.* (STAR Collaboration), arXiv: 0909.4131 [nucl-ex]; L. Kumar (for the STAR Collaboration) J. Phys. G **36** 064066 (2009); J. Y. Chen (for STAR Collaboration), arXiv: 0910.0556 [nucl-ex].
- [23] B. B. Back *et al.* (PHOBOS Collaboration), Phys. Rev. Lett. **97** 012301 (2006).
- [24] R. J. M. Snellings, H. Sorge, S. A. Voloshin, F. Q. Wang, and N. Xu, Phys. Rev. Lett. **84** 2803 (2000).
- [25] H. Liu, S. Panitkin and N. Xu, Phys. Rev. C **59** 348 (1998).
- [26] J. Brachmann *et al.*, Phys. Rev. C **61** 024909 (2000); L.P. Csernai and D.Rohrich, Phys. Lett. B **458** 454 (1999).

(Dated: November 5, 2018)

*Abstract*

